J Mater Sci
DOI 10.1007/s10853-011-6049-8

Phase transitions and hard magnetic properties for rapidly solidified MnAl alloys doped with C, B, and rare earth elements

Z. W. Liu · C. Chen · Z. G. Zheng · B. H. Tan · R. V. Ramanujan

Received: 15 June 2011 / Accepted: 13 October 2011

Abstract MnAl alloys are attractive candidates to potentially replace rare earth hard magnets because of their superior mechanical strength, reasonable magnetic properties, and low cost. In this study, the phase transitions and magnetic properties of melt spun $Mn_{55}Al_{45}$ based alloys doped with C, B, and rare earth (RE) elements were investigated. As-spun Mn–Al, Mn–Al–C, and Mn–Al–C–RE ribbons possessed a hexagonal ε crystal structure. Phase transformations between the ε and the $L1_0$ (τ) phase are of interest. The $\varepsilon \rightarrow \tau$ transformation occurred at $\sim$500 °C and the reversed $\tau \rightarrow \varepsilon$ transformation was observed at $\sim$800 °C. Moderate carbon addition promoted the formation of the desired hard magnetic $L1_0$ τ-phase and improved the hard magnetic properties. The Curie temperature T_C of the τ phase is very sensitive to the C concentration. Dy or Pr doping in MnAlC alloy had no significant effect on T_C. Pr addition can slightly improve the magnetic properties of MnAlC alloy, especially J_S. Doping B could not enhance the magnetic properties of MnAl alloy since B is not able to stabilize either the ε phase or the $L1_0$ hard magnetic τ phase.

Introduction

Hybrid cars and electric vehicles require increasing quantities of rare earth magnets, e.g., Dy-substituted $Nd_2Fe_{14}B$, $SmCo_5$, and $Sm_2Fe_{17}N$, because of their excellent magnetic properties. However, rare earth (RE) resources have become a major issue in the international community. Developing high performance permanent magnets without RE elements is therefore an urgent need. MnAl alloys are attractive candidates to replace rare earth permanent magnets because of their superior mechanical strength, excellent machinability, and reasonable magnetic properties. Importantly, these hard magnets are relatively low cost because they do not contain rare earth or other elements in limited supply such as Co and Ni. The hard magnetic properties of MnAl alloys derive from the formation of a $L1_0$ intermetallic phase (tetragonal τ-MnAl) characterized by strong, uniaxial magnetocrystalline anisotropy (10^6 J/m^3) with an easy *c*-axis [1–4]. Unfortunately, the τ phase is metastable, forming from a quenched-in high-temperature hexagonal (ε) phase by annealing at $\sim$550 °C [1]. The parent hexagonal disordered ε-phase is antiferromagnetic ($T_N = 97$ K) [5]. It has been found [6] that addition of small amounts of carbon stabilizes the τ phase and prevents the decomposition of the alloy into the stable but nonmagnetic γ (Al_8Mn_5) and β (Mn) phases. The stabilized τ-phase can also be obtained by slow cooling (<8 °C/min) from the temperature interval, where the ε-phase is stable (from above 800 °C) [1, 7].

The magnetic properties of Mn–Al–C alloys are dependent on the composition and microstructure, which is in turn strongly influenced by τ-phase formation [5]. Some previous investigations showed that an alloy with 1.7 at.% C has the best hard magnetic properties since the uniformly dispersed fine Mn_3AlC phase in the τ phase can pin the domain walls and improve coercivity [5, 8–10]. The best magnetic properties with maximum energy product $(BH)_{max}$ up to 64.4 kJ/m^3 have been reported in an anisotropic Mn–Al–C alloy obtained by high-temperature extrusion [11, 12].

Z. W. Liu (✉) · C. Chen · Z. G. Zheng
School of Materials Science and Engineering, South China University of Technology, Guangzhou 510640, China
e-mail: zwliu@scut.edu.cn

B. H. Tan · R. V. Ramanujan
School of Materials Science and Engineering, Nanyang Technological University, Singapore 639798, Singapore

Published online: 27 October 2011

Despite the above progress, MnAl-based alloys have not been fully studied and explored, possibly because of the existence of RE magnets (such as NdFeB and SmCo) with very good magnetic properties. There has not been much work on MnAl alloys except those focused mainly on MnAl thin films [13]. The previous literature also reveals inconsistent. Zeng et al. [14] investigated the MnAl base alloys produced by mechanical milling and subsequent annealing. A high coercivity of ~380 kA/m was obtained for nanostructured $Mn_{54}Al_{46}$ annealed at 400°C. They also obtained Curie temperatures T_C from 346 to 382 °C for Mn–Al binary alloys and 329 to 338 °C for MnAlC ternary alloys with 1.7 at.% C [9]. However, Fazakas et al. [7] investigated the $Mn_{54}Al_{44}C_2$ alloy synthesized by melt spinning followed by annealing and found very different results. The T_C of this alloy was only 247 °C and the coercivity was less than 103 kA/m, which is much lower than the values reported by Zeng et al. [10]. Except for this study, synthesis of MnAl-based hard magnetic alloys by rapid quenching has received almost no attention. The melt spinning is a feasible technique to prepare magnetic materials, such as NdFeB and SmCo alloys. This technique is useful in formation of nanostructures and is scalable for mass production as well as for fundamental investigations of phase transitions. Hence, melt spinning was used to prepare MnAl-based alloys in this study. The MnAl magnets with elemental additions other than C have been rarely studied. Hence, in this study, the phase transformations and the effect of heat treatment on MnAl(C) alloys prepared by melt spinning are investigated. RE elements (Pr and Dy) having 4f magnetism were used as dopants to improve the magnetic properties. In addition, substitution of C by B, another group IIA element, was also examined to elucidate its effects on the structure and properties.

Experimental

MnAl alloy ingots with various compositions, including $Mn_{55-x}Al_{45}C_x$ ($x = 0$, 1, 1.7 and 2), $Mn_{53.5}Al_{45}B_{1.5}$, and $Mn_{52.3}Al_{45}C_{1.7}RE_1$ (RE = Pr or Dy) were produced by argon arc melting. Special care has been paid to melting the alloys because of the large differences in the melting point and saturated vapor pressure of the raw materials (Mn, Al, and C). The as-prepared ingots were used to prepare ribbon samples by a single-roller melt spinning technique under protective atmosphere (argon) at a wheel speed of 40 m/s. The evolution of the microstructure of the as-spun samples was examined by X-ray diffraction (Philips, Cu Kα radiation). Differential scanning calorimetery (Perkin-Elmer TGA7) was employed to study the structural transformations in the temperature range of 300–1000 °C with a temperature ramp rate of 20 °C/min. The as-spun ribbons were annealed at 500–650 °C for 10 min under argon atmosphere. The magnetic properties at various temperatures were characterized by a physical properties measurement system (PPMS, Quantum Design Co.) equiped with a vibrating sample magnetometer (VSM), using an applied field of 5 T.

Results and discussion

Since it is difficult to control elemental loss during argon melting of Mn–Al–C based alloys, the compositions of as-spun ribbons were first examined by chemical analysis. All alloys discussed in this article were verified to have a very small difference (less than 1%) in the actual composition compared to their nominal compositions. The XRD patterns for as-spun ribbons with six compositions are shown in Fig. 1. For all Mn–Al, Mn–Al-C, and Mn–Al–C–RE compositions, the ribbons have a single phase structure consisting of the ε phase. The concentrations of C, Pr, and Dy had no effect on the phase structure of the as-quenched alloys. However, the $Mn_{53.5}Al_{45}B_{1.5}$ alloy contained β-Mn and γ-Al_8Mn_5 phases on addition to the majority ε phase. The result indicates that boron promotes the precipitations of β-Mn and γ-Al_8Mn_5 phases, which are stable at low temperature, from the parent ε phase during rapid quenching.

Thermal analysis was used to investigate the phase transition temperatures and to find a suitable annealing temperature regime for the as-quenched ribbons. The DSC results are shown in Fig. 2. Except for the $Mn_{53.5}Al_{45}B_{1.5}$ alloy, all compositions exhibit at least two phase transitions on heating from room temperature to 900 °C. For the

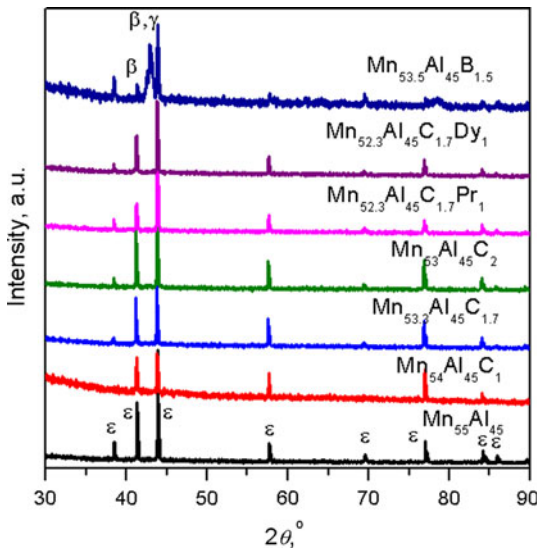

Fig. 1 XRD patterns for as-spun alloys with various compositions

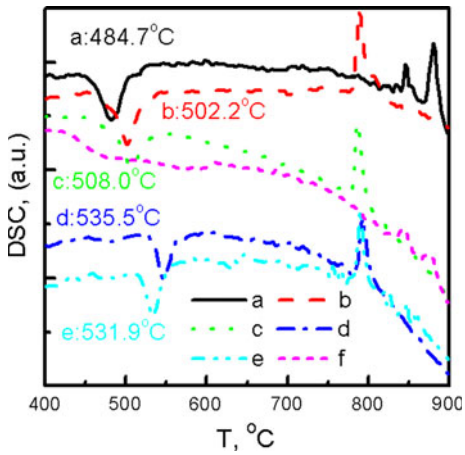

Fig. 2 DSC curves for experimental alloys: **a** $Mn_{55}Al_{45}$, **b** $Mn_{54}Al_{45}C$, **c** $Mn_{53.3}Al_{45}C_{1.7}$, **d** $Mn_{52.3}Al_{45}C_{1.7}Pr$, **e** $Mn_{52.3}Al_{45}C_{1.7}Dy$, **f** $Mn_{53.5}Al_{45}B_{1.5}$

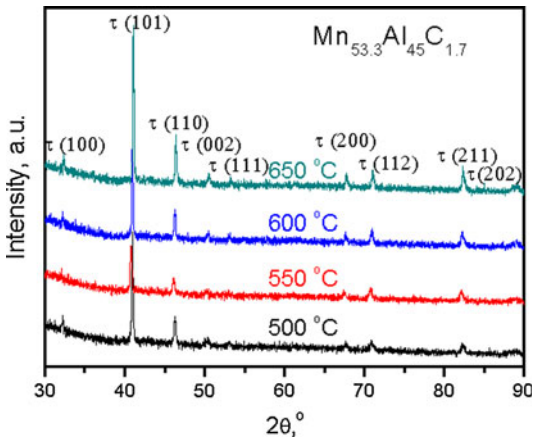

Fig. 3 XRD patterns for $Mn_{53.3}Al_{45}C_{1.7}$ alloys after annealing at various temperatures

$Mn_{55}Al_{45}$ alloy, one sharp exothermic peak at 484.7 °C was observed, corresponding to the structural transformation of the quenched-in ε-phase to the metastable magnetic τ-phase. The endothermic peak at ~850 °C corresponds to the transformation of the τ-phase back into the non-magnetic ε-phase. The endothermic peak at ~875 °C corresponds to the precipitation of the β phase and γ phase. For the C containing alloys, only two peaks appeared in the DSC curves, indicating that C can prevent the formation of β and γ phases. The first peak in the temperature range of 500–550 °C and the second peak at ~800 °C correspond to the $\varepsilon \rightarrow \tau$ and $\tau \rightarrow \varepsilon$ transformations, respectively. 1 at.% C addition reduces the $\tau \rightarrow \varepsilon$ transformation temperature from ~850 °C to less than 800 °C. It is also found that C and RE addition changes the $\varepsilon \rightarrow \tau$ transformation temperature but does not significantly affect the $\tau \rightarrow \varepsilon$ transformation temperature. C slightly increases the $\varepsilon \rightarrow \tau$ transformation temperature, Pr or Dy also shifts this transformation to higher temperatures. This shows that C can stabilize the τ-phase and prevent its decomposition into the β-Mn and γ-Al_8Mn_5 phases. As can be seen from the DSC results, for the $Mn_{53.5}Al_{45}B_{1.5}$ alloy, $\varepsilon \rightarrow \tau$ and $\tau \rightarrow \varepsilon$ transitions were almost absent. Two small peaks at ~850 and 875 °C can be the results of transitions of $\varepsilon \rightarrow \beta$-Mn and $\varepsilon \rightarrow \gamma$-$Al_8Mn_5$, respectively. The results imply that C substitution by B cannot promote the formation of τ phase from ε phase.

To prepare single phase alloys comprised solely of magnetic τ phase, all samples were annealed at 500–650 °C in argon atmosphere. Figure 3 shows the XRD patterns for the $Mn_{53.3}Al_{45}C_{1.7}$ alloys annealed at various temperatures. It is found that the $L1_0$ phase has formed at 500 °C when the sample were annealed for 10 min. Increased peak intensity at higher temperatures indicates that the crystallinity of the $L1_0$ phase is improved and the grain size increases with increasing annealing temperature. No other phase was observed for the alloy annealed in this temperature range. The XRD patterns for all compositions after annealing at 600 °C and for $Mn_{55}Al_{45}$ annealed at 550 °C are shown in Fig. 4. For the binary Mn–Al alloy, stable β and γ phases were detected. The alloys contain mixtures of the γ, β, and τ phases. It is evident that as temperature increases from 550 to 600 °C, the mass fractions of γ and β phases increase at the expense of the τ phase. The results clearly show that the τ phase decomposed into the stable γ and β phases in the MnAl alloy without C addition. This result is in good agreement with that observed by Zeng et al. [10]. Figure 4 thus indicates that a small amount of C addition indeed stabilizes the hexagonal metastable $L1_0$ phases. The ε phase decomposition into γ (Al_8Mn_5) and β(Mn) phases is prevented and the ε phase completely transformed into the hard magnetic τ phase [2]. Also, co-doping RE (Nd or Dy) with C did not change the crystal structure of MnAlC alloys after heat

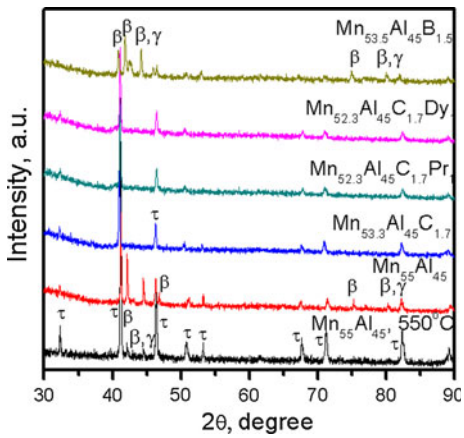

Fig. 4 XRD patterns for all alloys after annealing at 600 °C and for $Mn_{55}Al_{45}$ alloys after annealing at 550 °C

treatment. Furthermore, XRD results again indicate that B substitution for C in Mn–Al–C could not promote the transformation from ε phase to τ phase during annealing. In fact, B prevents the transition of $\varepsilon \rightarrow \tau$.

The magnetic properties of MnAlC alloys with various C concentrations annealed at various temperatures are shown in Fig. 5. The binary alloy $Mn_{55}Al_{45}$ has relatively low magnetic properties because of the mixture of the τ, β, and γ phases. C addition improves the hard magnetic properties because C stabilizes and promotes the precipitation of the τ phase, as discussed above. The high anisotropy field of the τ phase results in an increase in the coercivity. It is found that the MnAlC alloy with C content of 1.7 at.% has the best combination of magnetic properties, $J_S = 0.83$ T, $J_r = 0.30$ T, $H_{cj} = 123$ kA/m, and $(BH)_{max} = 12.24$ kJ/m^3 were obtained in alloys annealed at 650 °C. This is in good agreement with previous studies [9, 11]. The hysteresis loops for $Mn_{53.3}Al_{45}C_{1.7}$ alloys annealed at various temperatures are shown in Fig. 6. The J_r and $(BH)_{max}$ slightly increase with increasing annealing temperature, possibly because of the increased mass fraction of the hard magnetic phase. High coercivity for the alloy with 1.7 at.% C may also result from the precipitation of a small amount of Mn_3AlC phases inside the τ phase, which can pin the domain wall [9, 12]. For alloys containing 2 at.% C, the magnetic properties decrease when the annealing temperature is greater than 550 °C. The reason has been attributed to the fact that too much carbon is not beneficial to the nucleation and growth of τ phase [7]. The magnetic properties of both $Mn_{54}Al_{45}C$ and $Mn_{53}Al_{45}C_2$ alloys are inferior to those of $Mn_{53.3}Al_{45}C_{1.7}$

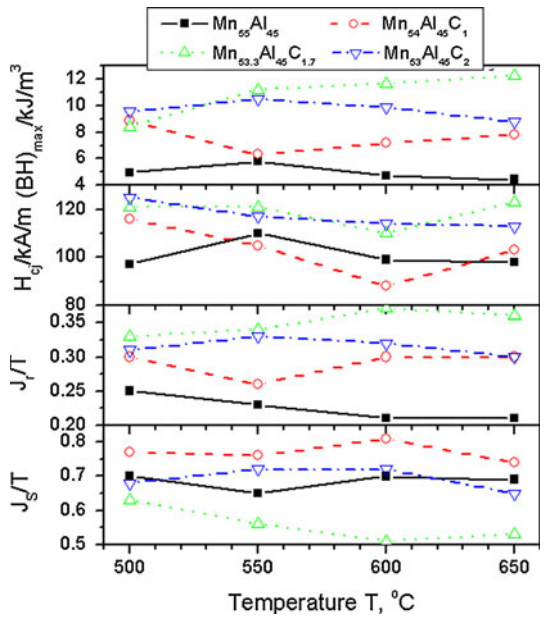

Fig. 5 Magnetic properties for MnAl(C) alloys with various C concentrations after annealing at various temperatures

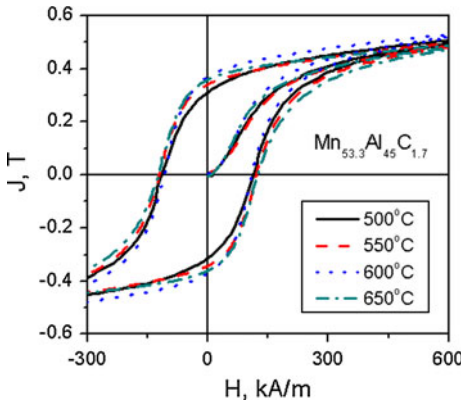

Fig. 6 Hysteresis loops for $Mn_{53.3}Al_{45}C_{1.7}$ alloys annealed at various temperatures

alloy, indicating that there is an optimized C concentration for the best magnetic properties.

Figure 7 shows the M–T curves for MnAlC alloys with various C contents after annealing at optimized temperatures. The Curie temperatures T_C can be determined from the inflection points of M–T curves, as indicated by the arrows. The results indicated that T_C is very sensitive to the C concentration. As shown in the inset of Fig. 7, a linear decrease of T_C with C concentration is observed. Adding 1, 1.7, and 2 at.% C to $Mn_{55}Al_{45}$ alloy reduce the T_c from 346 °C to 292, 268 and 258 °C, respectively. This large drop of T_C caused by C doping can explain the large discrepancy between the previous results obtained by Zeng et al. [10] and Fazakas et al. [7]., loss of carbon is likely to have occurred in Zeng's samples.

Figure 8 shows the effects of RE additions on the magnetic hysteresis loop of MnAlC alloy with C content of 1.7%. The results show that addition of Pr can slightly improve the J_s, J_r and $(BH)_{max}$ of $Mn_{53.3}Al_{45}C_{1.7}$ alloy, but the effect of Dy is not positive. The effects of RE on the

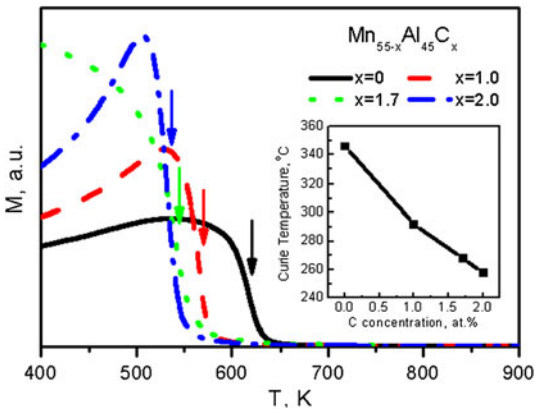

Fig. 7 M–T curves and Curie temperature (inset) for $Mn_{55-x}Al_{45}C_x$ alloys with various C contents after annealing at optimized temperatures

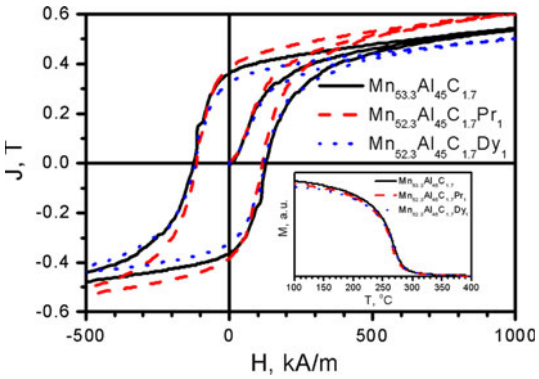

Fig. 8 Hysteresis loops and M–T curves for $Mn_{53.3}Al_{45}C_{1.7}$, $Mn_{52.3}Al_{45}C_{1.7}Pr$, and $Mn_{52.3}Al_{45}C_{1.7}Dy$ alloys after annealing at 650 °C for 10 min

MnAlC are possibly related to the large magnetic moment of RE elements. Further investigations are needed to clarify the underlying mechanisms. Figure 8 (inset) shows the M–T curves for the MnAlC alloys without and with RE doping. The T_C of the τ phase deduced from these curves shows a slight decrease from 268 to 264 °C or 267 °C for Pr or Dy additions, respectively.

Figure 9 shows the hysteresis loops at 5 K for all the alloys except the boron doped alloy after optimized annealing. It shows clearly the differences in J_S, J_r and ${}_jH_C$ for these alloys. C addition improves the saturation magnetization and coercivity of the MnAl binary alloys by promoting the formation of hard phase with large anisotropy. Pr and Dy doping further improves the anisotropy, which can be attributed to 3*d*–4*f* electron interactions or simply the increase in atomic distance between Mn atoms [15]. The best properties were obtained in C and Pr doped MnAl alloy.

The magnetic properties of melt spun Mn–Al based alloys are much lower than that reported for MnAlC

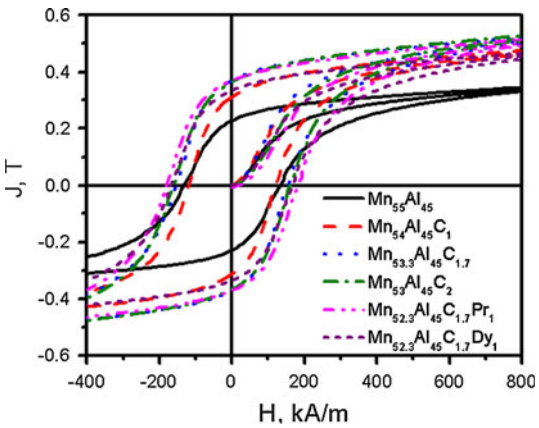

Fig. 9 Hysteresis loops at 5 K for experimental alloys after optimized heat treatment

magnets prepared by hot extrusion of annealed gas-atomized powders [11]; processing has an important effect on the microstructure and properties. Zeng et al. [10] also suggested that the magnetic hysteresis behavior of Mn–Al–C is extremely sensitive to the microstructure and defects introduced during the formation of the τ-phase within the high-temperature ε-phase. High hard magnetic properties for commercial products produced by hot extrusion are a result of high anisotropy, grain size reduction and carbide precipitations. The coercivities of our samples are also lower compared to those obtained by Zeng [10] from ball milled MnAlC samples. However, as indicated earlier, the magnetic properties obtained in this work are very close to these obtained by Fazakas et al. [7] using the same preparation method of melt spinning. The difference in the properties between melt spun and ball milled alloys could result from these two distinct preparation methods, which lead to different grain structures and defects. It is not easy to achieve nanostructures in MnAl alloys by melt spinning because of the low glass formability of this alloy. We believe that the magnetic properties can be improved by reducing grain size and inducing anisotropy. The results thus indicated that an appropriate processing technique and treatment process has to be developed for making full use of this low cost permanent magnet.

Conclusions

As-quenched MnAl alloys with C doping or C and RE additions exhibits a single phase structure, consisting of the hcp ε phase. After annealing at suitable temperatures, ε can transform to the metastable ferromagnetic τ phase. The effects of composition and heat treatment on the phase transition and hard magnetic properties have been investigated. Addition of C is beneficial to the formation of the τ phase and, thus to the hard magnetic properties. C content also has a significant effect on the T_C of τ phase. 2% C addition reduced the T_C from 346 to 258 °C. The $Mn_{53.3}Al_{45}C_{1.7}$ ribbon after annealing at 650 °C for 10 min has the best combined magnetic properties. Doping of rare earth elements Pr can slightly improve the hard magnetic properties, but Dy does not have a positive effect. B does not stabilize the hard magnetic phase, the unstable ε phase transform to intermediate phases during annealing. Our results indicated that the properties of MnAl-based alloys depend strongly on the processing method.

Acknowledgement This study is partly supported by the Natural Science Foundation of China (Grant Nos. 50874050 and 51174094) and the Fundamental Research Funds for the Central Universities, SCUT (Grant No. 2009ZZ0025). ZWL also thank the School of Materials Science and Engineering at the Nanyang Technological University for a visiting professorship.

References

1. Kamino K, Kawaguchi T, Nagakura M (1966) IEEE Trans Magn 2:506
2. Yanar C, Wiezorek JMK, Radmilovic V, Soffa WA WA (2002) Metall Mater Trans A 33:2413
3. Loch AJJ, Hokkeling P, Sterg MGVD, DeVos KJ (1960) J Appl Phys 31:75S
4. Sakka Y, Nakamura M, Hoshimoto K (1989) J Mater Sci 24:4331. doi:10.1007/BF00544507
5. Wyslocki JJ, Pawlik P, Przybyl A (1999) Mater Chem Phys 60:211
6. Yang YC, Ho WW, Lin C, Yang JL, Zhou HM, Zhu JX, Zeng XX, Zhang BS, Jin L (1984) J Appl Phys 55:2053
7. Fazakas E, Varga LK, Mazaleyrat F (2007) J Alloys Comp 434–435:611
8. Kono H (1958) J Phys Soc Japan 13:1444
9. Ohtani T, Kato N, Kojima K, Sakamoto Y, Konno I, Tsukahara M, Kubo T (1977) IEEE Trans Magn 13:1328
10. Zeng Q, Baker I, Cui JB, Yan ZC (2007) J Magn Magn Mater 308:214
11. Yamaguchi A, Tanaka Y, Yanagimoto K, Sakaguchi I, Kato N (1989) Bull Jpn Inst Met 28:422
12. Pareti L, Bolzoni F, Leccabue F, Ermakov AE (1986) J Appl Phys 59:3824
13. Yan ZC, Huang Y, Zhang Y, Hadjipanayis GC, Soffa W, Weller D (2005) Scripta Mater 53:463
14. Zeng Q, Baker I, Yan ZC (2006) J Appl Phys 99:08E902
15. Bohlmann MA, Koo JC, Wise JH (1981) J Appl Phys 52:2542